**ARTICLE**

# Dielectric spectroscopy investigation of relaxation processes in the low-frequency regime and validity of the Stokes–Einstein–Nernst/Stokes–Einstein–Debye relation in poly(propylene glycol)

Lokendra P. Singh[1,2] · Gagan Sharma[2]

## Abstract

Relaxation processes over the static permittivity frequency region present in poly(propylene glycol) [PPG] of average molecular weights $M_n = 425$ and 725 have been investigated in the temperature range (285–320 K) and frequency range (1 Hz–1 MHz) using broadband dielectric spectroscopy. The data have been compared in the form of complex dielectric permittivity ($\varepsilon^*$), electric modulus ($M^*$), conductance ($\sigma^*$), and impedance ($Z^*$) spectra of PPG. From the comparative analysis of the spectra of all the complex quantities, the temperature-dependent relaxation processes caused by the presence of electrode polarization and ionic conduction effects were explored. The temperature dependence of various dielectric parameters such as dc conductivity ($\sigma_{dc}$), relaxation time due to electrode polarization ($\tau_{EP}$), conductivity relaxation time ($\tau_\sigma$), and their activation energies have been critically examined. It was observed that the dependence of dc conductivity ($\sigma_{dc}$) on the viscosity ($\eta$) or structural relaxation time ($\tau_\alpha$) of both PPGs satisfies the Stokes–Einstein–Nernst/Stokes–Einstein–Debye quite well. This behavior is similar to those reported in lithium percolate (LiClO$_4$) electrolyte solutions in PPG solvents. This demonstrates that the electrical conduction behavior of unknown ions impurities existing in pure PPG and extremely low known concentration added ions in pure PPG is the same.

✉ Lokendra P. Singh
   drlokendrapratapsingh@mits.ac.in; lps.jnu@gmail.com

1   Department of Physics, Madanapalle Institute of Technology
    & Science, Madanapalle 517325, Andhra Pradesh, India

2   Department of Physics, Lovely Professional University,
    Phagwara, Punjab 144411, India

**Graphical abstract**
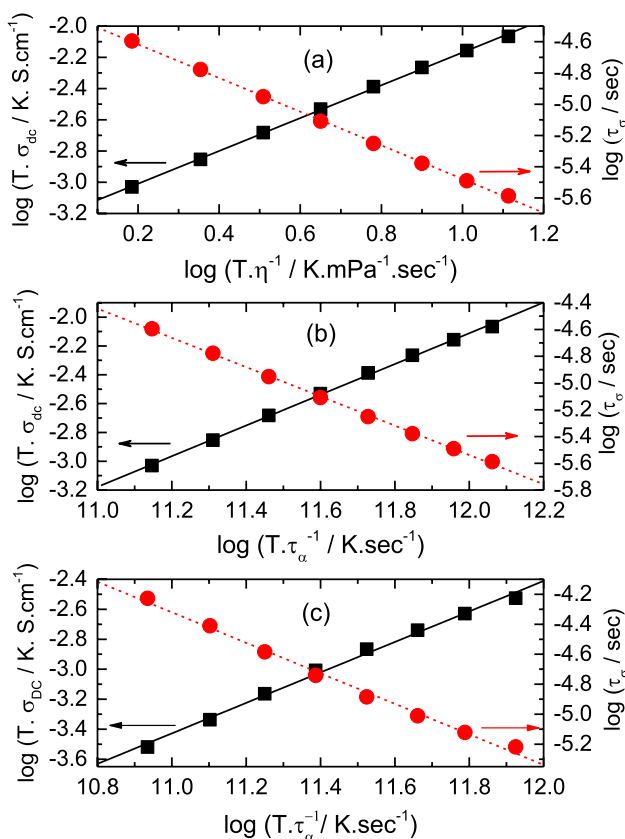


**Keywords** Poly(propylene glycol) · Dielectric properties · Ionic conductivity · Relaxation processes · Activation energies · Stokes–Einstein relation

# 1 Introduction

Liquid polymers play an important role in our daily life due to their exceptional variety of properties. Among various polymers, poly(propylene glycols) (PPGs) play an important role in the industry's applications such as in making capacitors, pharmaceuticals, and anti-foaming agents in fermentation as well used as plasticizing agents. Due to their large applications, PPG of different molecular weights has been investigated extensively by different research groups using different techniques such as dielectric spectroscopy [1–11], mechanical spectroscopy [11–13], NMR spectroscopy [14, 15], photon correlation spectroscopy [16], and light scattering [17]. The first systematic dielectric studies of pure PPG of different molecular weights down to glass transition temperature were carried out by Baur and his co-researchers [2]. Later, PPGs of different molecular weights were widely investigated by several researchers using dielectric spectroscopy [3–11]. For example, Suzuki et al. [18]

studied the temperature- and pressure-dependent dielectric relaxation behavior of PPG with different molecular weights and terminal groups. Sengwa et al. [19] studied the effect of various solvents on the relaxation times of PPG-2000 using microwave dielectric relaxation spectroscopy. Park et al. [20, 21] studied the thermal and dielectric properties of propylene glycol and poly(propylene glycol) with different molecular weights. Using quasielastic neutron scattering, Swenson et al. [22] investigated the dynamics of propylene glycol (PG) and poly(propylene glycol) (PPG). To explain the variations in relaxation mechanism with increasing chain length, Ikada et al. [23, 24] have attempted to investigate the relationship between the dielectric behavior and molecular structures of oligomers of ethylene and propylene glycols. Grzybowska et al. [25] identified various relaxation processes in PPG-400 down to glass transition temperature using broadband dielectric spectroscopy. Moreover, Singh et al. [26] have studied the relaxation dynamics of water in PPG solutions with different concentrations at various temperatures using broadband dielectric spectroscopy. Furthermore, using Brillouin scattering and temperature-modulated DSC, Koda et al. [27] investigated the acoustic and thermal characteristics of the liquid glass transitions of propylene glycol and its oligomers.

Comparing different experimental tools, dielectric/impedance spectroscopy is one of the most widely used techniques to study the behavior of these kinds of polar materials because of covering the frequency range from μHz to THz [28]. In polar materials, the ionic conduction and electrode polarization phenomena take place towards the lower frequency side of dielectric spectra, whereas inter- and intra-molecular reorientation dynamics are responsible for the high-frequency dielectric dispersion [28]. In most of the dielectric studies, PPG exhibits the dielectric signature of structural relaxation process (α-process) of non-Debye type, secondary relaxation process along with the dc conductivity due to free ions towards the low-frequency side [23–26]. The existence of free ions is very common in liquid polar dielectric materials, which are responsible for the occurrence of low-frequency dielectric dispersion [28–36]. Moreover, the electrode polarization (EP) phenomenon is one of the most undesired effects which occur due to the blocking of charges at the interface of dielectric material and the metallic electrode surface of the cell [28, 29]. It has been observed that the characteristics of relaxation processes observed in the low-frequency regime of PPGs, or other dipolar liquids are almost similar to those observed in liquid polymeric electrolyte solutions [37–39]. Most dipolar liquids possess the existence of these unidentified free ions which are further activated with the help of some electromagnetic irradiations [40, 41]. The characteristics of these unidentified free ions in liquid, as well as solid electrolytes, have been mostly explored by using low-frequency dielectric/impedance

spectroscopy [36–38, 42]. Hence, it is interesting to explore thoroughly the temperature-dependent dielectric and electrical behavior of pure PPG using low-frequency dielectric relaxation spectroscopy (DRS), which are important from a technological, industrial, and academic point of view. Furthermore, it would be intriguing to compare our experimental results with the predictions of the Stokes–Einstein and Stokes–Einstein–Debye models, that correlate the diffusion coefficients, given in the quasi-macroscopic hydrodynamic approximation obtained from the Stokes theory [43] to the microscopic quantities. According to the Nernst–Einstein [44] relation, the translational diffusion coefficient or diffusion coefficient of ion ($D_i$) of the medium is linked with the mobility of ions ($\mu_i$) in the following way [44, 45]:

$$D_i = \frac{\mu_i k_B T}{q} = \frac{\sigma_{dc} k_B T}{n_i q^2} \tag{1}$$

where $\sigma_{dc}$ is the ionic dc conductivity, $k_B$ is the Boltzmann constant, $n_i$ represents the number density of ions and $q$ is the net charge on the ions. Similarly, one can drive the following relation between diffusion coefficient of ion ($D_i$) and viscosity ($\eta$) using Stokes theory as [43–45]

$$D_i = \frac{k_B T}{6\pi\eta r_i} \tag{2}$$

Here, $r_i$ is the radius of the ion. Using Eqs. (1) and (2), one drives the relation between the ionic dc conductivity ($\sigma_{dc}$) and viscosity ($\eta$) known as the Stokes–Einstein–Nernst relation [44, 45]:

$$\sigma_{dc} = \frac{n_i q^2}{6\pi\eta r_i} \tag{3}$$

Hence, the ionic dc conductivity ($\sigma_{dc}$) varies as the inverse of viscosity. This equation assumes that the solvent is a continuum and only deals with the Brownian diffusion of ions.

On the other hand, the rotational diffusion coefficient ($D_r$) and the average dielectric relaxation time usually known as structural relaxation time ($\tau_s$) for molecular dipole reorientations are connected by the Stokes–Einstein–Debye model [35, 44, 45] as

$$D_r = \frac{k_B T}{6\pi\eta r_d^3} \propto \frac{1}{\tau_s} \tag{4}$$

where $r_d$ is the radius of a dipolar molecule. The above equation suggests that the dc conductivity ($\sigma_{dc}$) is inversely proportional to the average dielectric relaxation time ($\tau_s$). The validity of the above equations has been discussed by several researchers [32–42, 45] working on molecular glass-forming liquids as well as polymers. For low viscous glass-forming materials, the above equation has been thoroughly validated.



**Fig. 1** Dielectric behavior of poly(propylene glycol) [PPG]: panels **a** and **b** show the frequency variation of real and imaginary part of permittivity at various temperatures for PPG ($M_n = 425$) while panels **c** and **d** represent the frequency variation of real and imaginary part of permittivity at various temperatures for PPG ($M_n = 725$). The inset in panels **a** and **c** show the magnified portion of the real part of permittivity ($\varepsilon'$) at higher frequencies of PPG-425 and PPG-725 respectively
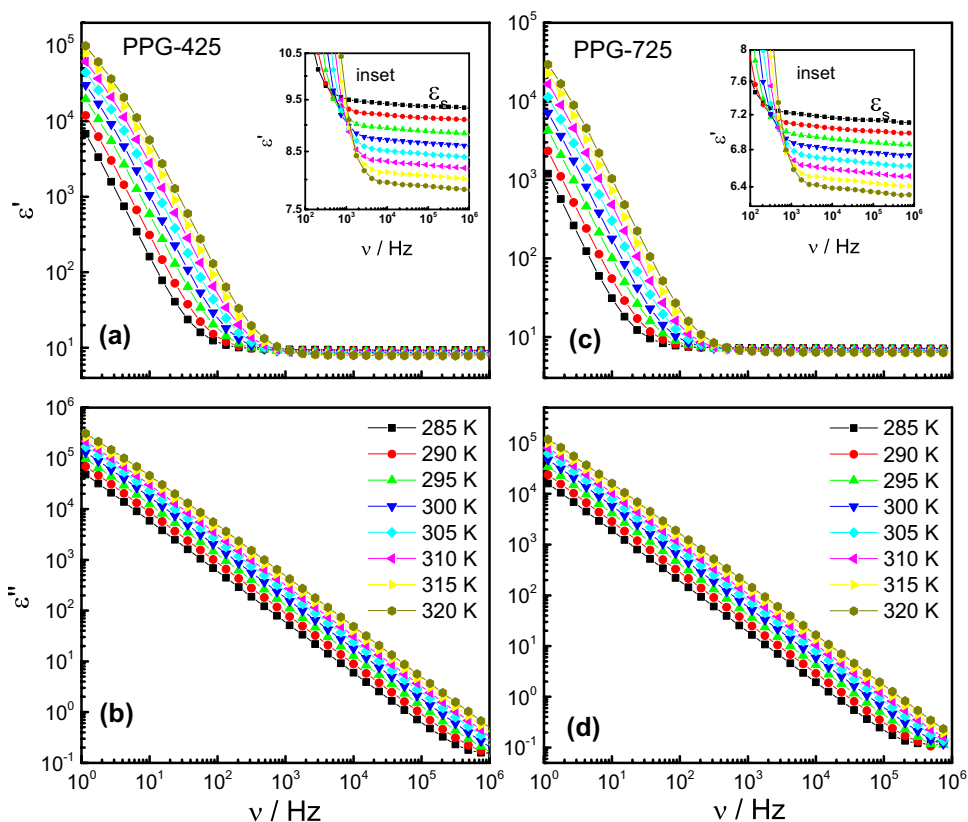
However, the Stokes–Einstein–Debye/Stokes–Einstein [32, 45] rule is broken in many glass-forming liquids with high viscosity, particularly when they approach towards the glass transition ($T_g$).

In the present article, we have attempted to characterize the comparative dielectric and electrical behavior of PPG concerning ionic and electrode polarization phenomena (EP) in the frequency range 1 Hz to 10 MHz and range of temperatures from 285 to 320 K. The temperature dependence of the relaxation times of the above-mentioned dielectric phenomena are analyzed using the Arrhenius equation and their activation energies are estimated. Moreover, an attempt has been made to reveal the validity of Eqs. (3) and (4), i.e., Stokes–Einstein–Nernst and Stokes–Einstein–Debye relation between the dc conductivity ($\sigma_{dc}$) and the structural relaxation time constant ($\tau_\alpha$)/viscosity of pure PPG. Furthermore, the ion transport mechanism in pure PPG results has been compared with the binary electrolyte solutions of lithium percolate in PPG solvents [39].

## 2 Experimental

Poly(propylene glycol) of molecular weight $M_n = 425$ (purity ≥ 99.6%) and 725 gm/mol (purity ≥ 99%) have been purchased from Sigma-Aldrich and used without any further purification. To perform the dielectric measurement, a broadband dielectric spectrometer based on a Novocontrol alpha analyzer has been used to measure the real and imaginary part of the complex dielectric function, $\varepsilon * (\omega) = \varepsilon'(\omega) - i\varepsilon''(\omega)$ with $\omega = 2\pi\nu$, in the frequency range of 1 Hz ≤ $\nu$ ≤ 1 MHz. The liquid polymer sample (PPG) was introduced in between two parallel gold-plated electrodes with a diameter of 30 mm and 50 μm Teflon spacers were used to define the polymer thickness. After cooling the polymer sample at a rate of 10 K/min, the recording of frequency-dependent dielectric spectra was done at a fixed temperature during heating from T = 285 to 320 K with every 5 K steps. The stability of the sample temperature was found to be better than ± 0.1 K in the entire set of measurements. For further information about the experimental setup, the researcher may consult our earlier reference [46].

## 3 Results and discussion

Depicted in Fig. 1 are the frequency variation of ε′ and ε″ spectra of pure PPGs of average molecular weights $M_n = 425$ and 725 at various temperatures. On closer inspection of the real part of permittivity spectra (ε′), two characteristic frequency regions can be observed in the measured frequency (1 Hz to 1 MHz) and a temperature range from 285 to 320 K, where ε′ values show different behavior. For instance in

PPG-425, the first region, i.e., below 500 Hz, the real part of permittivity (ε′) values increases sharply by several orders of magnitude with the decrease of frequency. This sudden increase of the real part of permittivity (ε′) values with the decrease of frequency is due to the effect of electrode polarization (EP) which is dominated over the bulk properties. In the frequency region where the electrode polarization (EP) phenomenon appears, there is the formation of electric double layers capacitances by the accumulation of free charges and long-distance drifted ions at the sample and metallic electrode interfaces [28, 29]. Due to the formation of electric double-layer capacitances, the capacity of the cell increases rapidly, and hence as a result an apparent increase of the real part of permittivity (ε′) can be observed. Moreover, the rapid rise of ε′ towards the low-frequency side is also supporting the presence of a significant concentration of ionic impurities in pure PPG. Furthermore, at a fixed frequency, it is observed that the value of the real part of permittivity (ε′) increases rapidly with an increase in temperature in the region where the electrode polarization effect dominates. For example, in PPG-425, the value of ε′ at 285 K is about 12, whereas at 320 K, the observed value is around 104 at 100 Hz. Similarly, in PPG-725, the ε′ value varies from 7.4 to 96 from the low temperature (285 K) to high temperature (320 K) at the same frequency, i.e., at 100 Hz (see Fig. 1c). This suggests that the concentration of ions in electric double layers increases with the increase of temperature of pure PPG.

In the second region, i.e., above 500 Hz in PPG-425 and above 200 Hz in PPG-725, the long-range movement of free charges is restricted in PPG because of the development of fast charges in the stimulating ac electric field, and hence, as a result, the steady-state region is observed in the frequency-dependent ε′ spectra as can be seen in the inset of Fig. 1a and c, respectively. This suggests that the length of electric double layers at the sample and electrode interfaces decreases gradually with an increase in frequency, and at higher frequencies, it reduces completely [28, 29], in that way, the ε′(ν) values become equal to the static permittivity $\varepsilon_s$. The magnified portion of ε′(ν) curves at the higher frequency region are depicted in the inset of Fig. 1a and c for PPG-425 and PPG-725, respectively. Further inspection of the inset of Fig. 1 a reveals that, above 500 Hz, the real part of permittivity values is almost constant with frequency and these values slightly decrease with the increase of the temperature of PPG-425. Similar behavior of ε′(ν) curves shown in the inset of Fig. 1c can also be identified in PPG-725 above 200 Hz. The observed temperature-dependent static permittivity, $\varepsilon_s(T)$, values of pure PPG-425 are consistent with those reported by one of the present authors Singh et al. [26] of pure PPG-425 as well as observed by other researchers [39] in the case of PPG/LiClO₄ electrolyte solutions, which confirms that the concentration of unidentified ionic
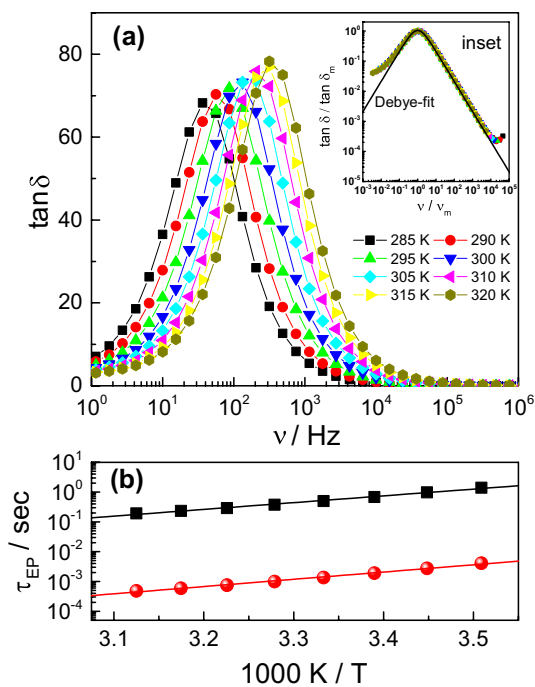
**Fig. 2 a** Frequency-dependent loss tangent (tan δ) spectra of pure PPG-425 at different temperatures. Inset depicts the variation of normalized loss tangent (tan δ/tan δ_m) as a function of normalized frequency (ν/ν_m) at different temperatures. Here, ν_m represents the maximum frequency at which the loss tangent curves show maximum value (tan δ_m) at a particular temperature. The solid line represents the Debye fit to the spectra. (b) Activation plot of time constant of electrode polarization (τ_EP) for PPG-425 (solid sphere) and PPG-725 (solid square). The solid lines along τ_EP are the best fits for the Arrhenius equation (Eq. 6)

impurity does not affect the static permittivity ($\varepsilon_s$) of pure PPG. In addition, it has been observed that the frequency value at which the steady-state region is observed in the spectrum of the real part of permittivity, $\varepsilon'(\nu)$, depends on the concentration of ionic impurity present in dipolar materials [31, 35, 36].

In a log–log scale, the dielectric absorption spectra $\varepsilon''(\nu)$ of pure PPG decrease linearly with an increase of frequency with a slope approximately equal to one at all measured temperatures as can be seen in Fig. 1b and d. This behavior suggests that the ionic current in both pure PPGs follows Ohm's law where the current density is a linear function of the strength of the electric field [28]. For the liquid dielectric materials of Ohmic behavior, their dielectric loss $\varepsilon''(\omega)$ spectrum follows a linear relation given by [28, 33]

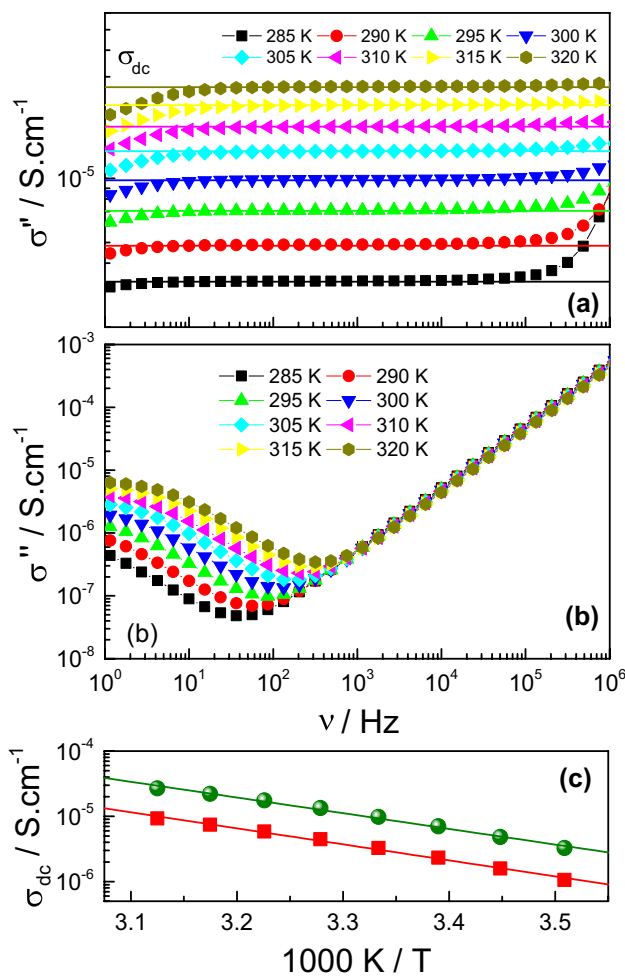$$\varepsilon''(\omega) = \frac{\sigma_{dc}}{\omega.\varepsilon_0} \qquad (5)$$



**Fig. 3** Frequency-dependent of real ($\sigma'$) and loss part ($\sigma''$) of ac conductivity of pure PPG-425 at different temperatures are depicted in panels **a** and **b**, respectively. The solid lines drawn in $\sigma'$ spectra represent $\sigma_{dc}$ (T) values. Panel **c** depicts the activation plot of dc ionic conductivity ($\sigma_{dc}$) for PPG-425 (solid sphere) and PPG-725 (solid square). The solid lines in panel **c** are the best fits to the Arrhenius equation (Eq. 8)

albeit with different physical parameters. In Eq. 5, $\sigma_{dc}$ is the dc ionic conductivity, $\omega = 2\pi\nu$ represents angular frequency, and $\varepsilon_0 \approx 8.854 \times 10^{-12}$ F/m is the permittivity in free space. This behavior was also observed in most of the dipolar liquids [32–35] and diluted electrolyte solutions [31, 36–40]. However, the deviation of Eq. 5 is observed for some high molecular weight polymers. Furthermore, from Fig. 1b and d, one can identify that the dielectric loss $\varepsilon''$ of pure PPG increases with the increase of temperature at a fixed frequency, which is similar to its semiconducting-type electrical behavior. To get more information about the dielectric behavior of pure PPG towards the low-frequency side, the loss tangent (tan δ = $\varepsilon''/\varepsilon'$) spectra of PPG-425 at various temperatures are depicted in Fig. 2a.

This figure reveals the existence of relaxation peaks in between the frequency range from 40 to 500 Hz.

Similarly in PPG-725, the relaxation peaks related to electrode polarization exist in between the frequency range from 15 to 200 Hz. Interestingly, in both polymers (PPG-425 and PPG-725), the magnitude of these relaxation peaks increases and also shifts towards the higher frequency side with the increase of temperature. These observed relaxation peaks correspond to the electrode polarization relaxation processes usually known as electric double layers (EDLs) dynamics [28, 29, 35, 39]. To give the reader an idea about the temperature dependence of spectral shape, the normalized loss tangent (tan $\delta$/tan $\delta_m$) as a function of normalized frequency ($\nu/\nu_m$) is depicted in the inset of Fig. 2a. This figure suggests that all measured spectra of pure PPG-425 of different temperatures are overlapping. The overlapping of data points of all spectra at different temperatures in this scaled figure indicates that the electric double-layer (EDL) dynamical process in pure liquid PPG-425 occurring at different time scales exhibits the same activation energy, and also, the distribution of this relaxation time does not depend on temperature. Similar behavior is also observed for PPG-725. Furthermore, the time constant corresponding to the electrode polarization ($\tau_{ep}$) is obtained from the relation $\tau_{ep} = (2\pi \nu_m)^{-1}$, where $\nu_m$ is the frequency value at which tangent loss becomes maximum (tan $\delta_m$) at a particular temperature. The temperature-dependent relaxation times corresponding to the electrode polarization effects in both PPGs are depicted in Fig. 2b. In both studied polymers, viz., PPG-425 and PPG-725, the $\tau_{ep}$ value decreases with the increase of temperature thereby described by the well-known Arrhenius equation given by [47]

$$\tau_{ep} = A \exp\left(\frac{E}{RT}\right) \tag{6}$$

in which $A$ is a pre-exponential factor, $R$ ($= 8.314$ J/mol K) is the gas constant, $T$ is the absolute temperature, and E is an activation energy corresponding to the relaxation time. In Fig. 2b, the solid spheres and solid squares represent the relaxation time results due to electrode polarization for PPG-425 and PPG-725, respectively. The solid lines along each symbol represent fits to the Arrhenius equation, i.e., Eq. 6. The Arrhenius fit parameters are obtained as log A = − 10.96, − 7.85 and E or $E_{\tau(ep)} = 46.6 \pm 1.4$ kJ/mol, $43.48 \pm 1.3$ kJ/mol for PPG-425 and PPG-725 respectively. To get more information about the relaxation processes present over the static permittivity frequency region, the real ($\sigma'$) and imaginary parts ($\sigma''$) of complex ac electrical conductivity are determined from the relation [28] given by

$$\sigma^*(\omega) = \sigma'(\omega) + i\sigma''(\omega) = i\omega\varepsilon_0\varepsilon^*(\omega) = \omega\varepsilon_0\varepsilon''(\omega) + i\omega\varepsilon_0\varepsilon'(\omega) \tag{7}$$
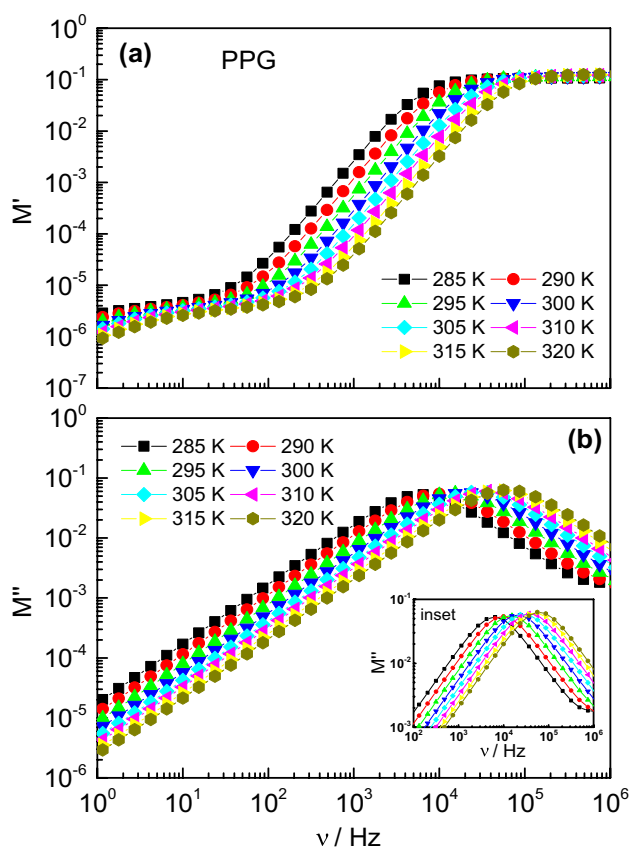


**Fig. 4** Variation of **a** real (M′) and **b** imaginary part (M″) of complex electrical modulus as a function of the frequency of pure poly(propylene glycol) [PPG-425] at different temperatures. The inset in panel **b** shows the magnified portion of the imaginary part of the electrical modulus (M″) at higher frequencies

in which the symbols have their usual meaning. The real ($\sigma'$) and imaginary parts ($\sigma''$) of ac electrical conductivity spectra obtained from the above Eq. 7 at different temperatures for PPG-425 are depicted in Fig. 3. The plateau region that exists in the spectra of the real part of ac electrical conductivity ($\sigma'$) gives the value of dc ionic conductivity ($\sigma_{dc}$) which is marked by solid lines as can be seen in Fig. 3a for PPG-425. The temperature dependence of dc ionic conductivity ($\sigma_{dc}$) obtained from the plateau region of $\sigma'(\nu)$ curves of both PPGs are presented in Fig. 3c. Clearly, the $\sigma_{dc}$ value increases with the increase of temperature which confirms the thermally activated behavior of unidentified ion impurities present in both PPGs. The activation energy of this process is obtained from the Arrhenius Eq. [47] of the form given by

$$\sigma_{dc} = A \exp\left(-\frac{E_{\sigma(dc)}}{RT}\right) \tag{8}$$

The activation parameters obtained from Eq. 8 are log A = 2.94, 2.69 and $E_{\sigma(dc)}$ = 46.01 ± 1.5 kJ/mol, 47.2 ± 1.4 kJ/mol for PPG-425 and PPG-725 respectively. Further, closer inspection of Fig. 3b reveals that the $\sigma''(\nu)$ spectra of pure PPG-425 initially decrease with the increase of frequency and reach minimum values in the frequency range 40 Hz–500 Hz, and then increase with the increase of frequency.

It is also observed that below the frequency where $\sigma''(\nu)$ spectra exhibit maximum dip, the values of $\sigma''(\nu)$ increase with the increase of temperature whereas above the maximum dip frequency these values increase linearly and are found to be independent of temperature. The frequency value at which the $\sigma''(\nu)$ spectrum shows maximum dip is the same as that of the tan δ peak frequency shown in Fig. 2a. This suggests that the relaxation process due to electrode polarization in dipolar materials can also be explored with the help of the frequency-dependent imaginary part of ac electrical conductivity, $\sigma''(\nu)$ spectrum.

Depicted in Fig. 4 are the frequency-dependent real (M′) and imaginary part (M″) of complex electric modulus of pure PPG-425 at various temperatures. This electric modulus formalism is commonly used to identify the conductivity relaxation process in dipolar liquids [31, 35, 36] and in electrolyte materials [37–39, 42] as it is free from the effect of electrode polarization due to relation $\varepsilon^*(\omega).M^*(\omega) = 1$, and also does not depend on the material of the measuring cell. Clearly, the frequency range (< 500 Hz) where electrode polarization effects are dominated shows a very small increase in the values of the real part of the electrical modulus (M′) in the pure PPG-425. This is because modulus

formalism suppresses high capacitance phenomena, whereas ε′ values are quite high in the same frequency range. But above this region (> 500 Hz), the values of M′ increase by several orders of magnitude with an increase of frequency, and finally, reach the steady-state values towards the high-frequency side as can be seen in Fig. 4a. This behavior is consistent with the results obtained for PPG-725 as well as those reported for dipolar liquids [35] and electrolyte solutions [30, 36, 39]. Moreover, Fig. 4b reveals that in a log–log scale, the imaginary part of the electrical modulus, M″(ν), increases linearly with the increase of frequency until the Debye-type relaxation processes are observed in the high-frequency region. These Debye-type relaxation peaks correspond to the ionic conductivity relaxation process as analyzed and discussed by several researchers for various dielectric liquids [36–42]. Furthermore, the magnitudes of these M″(ν) relaxation peaks increase gradually as well as a shift towards the high-frequency side with the increase of temperature of pure PPG can be identified in the inset of Fig. 4b. The frequency-dependent imaginary part of electrical modulus (M″) spectra are analyzed using the Debye function of the form given by [30]

$$M^*(\omega) = M_\infty + \frac{M_s - M_\infty}{1 + i\omega\tau_\sigma} \qquad (9)$$

where $M_s$ is defined as the inverse of static permittivity ($1/\varepsilon_s$), $M_\infty$ represents the inverse of high-frequency dielectric permittivity ($1/\varepsilon_\infty$), and $\tau_\sigma$ is the ionic conductivity relaxation time.

**Fig. 5** Activation plots of **a** conductivity relaxation time ($\tau_\sigma$) for PPG-425 (solid sphere) and PPG-725 (solid square), **b** structural relaxation time ($\tau_\alpha$) taken from reference (26) and (27) for PPG-425 and PPG-725, respectively. **c** Viscosity ($\eta$) data taken from reference (48) of pure PPG-425. The solid lines in each panel are the best fits to the Arrhenius equation
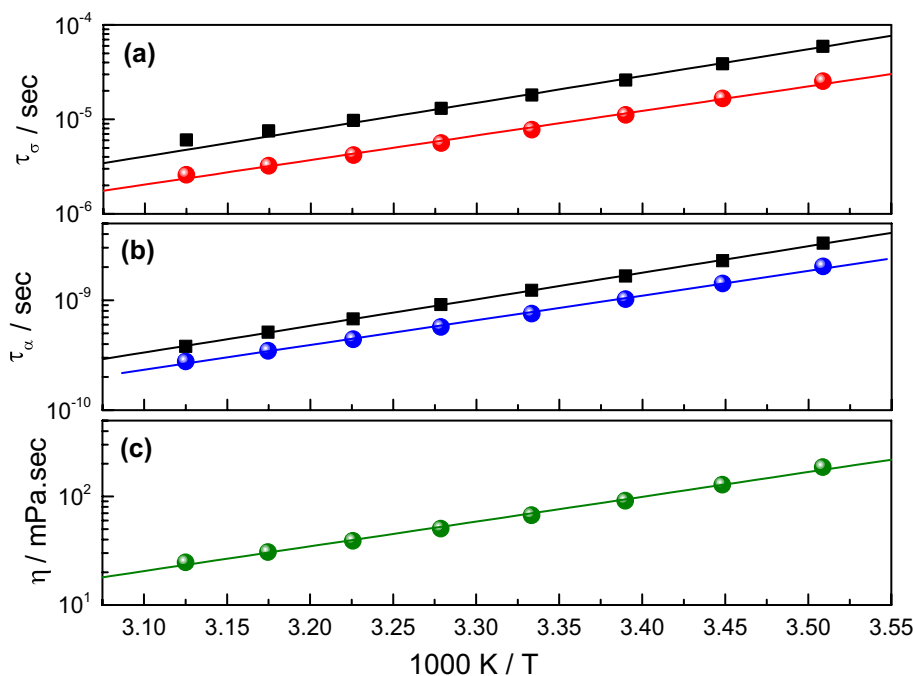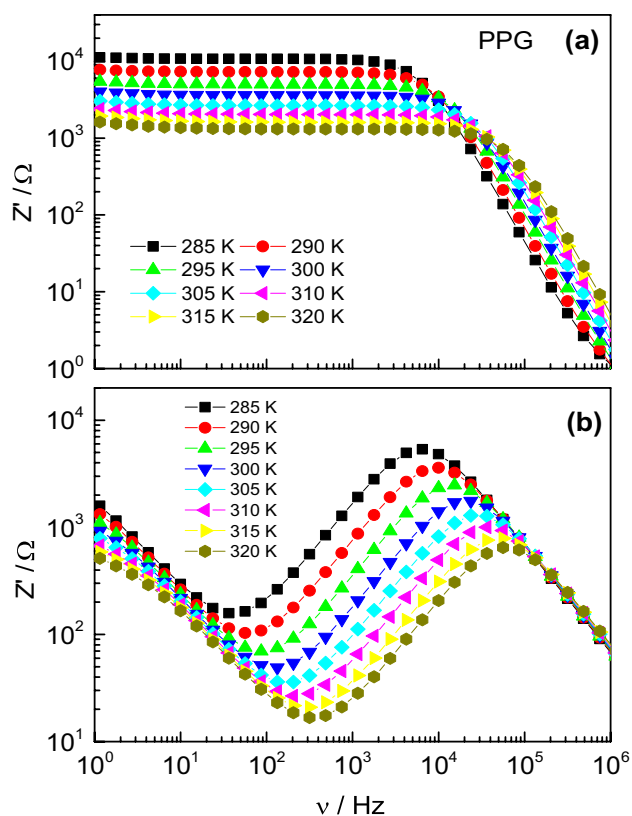
**Fig. 6** Frequency-dependent of **a** real (Z′) and **b** reactive part (Z″) of the complex impedance of pure poly(propylene glycol) [PPG-425] at different temperatures
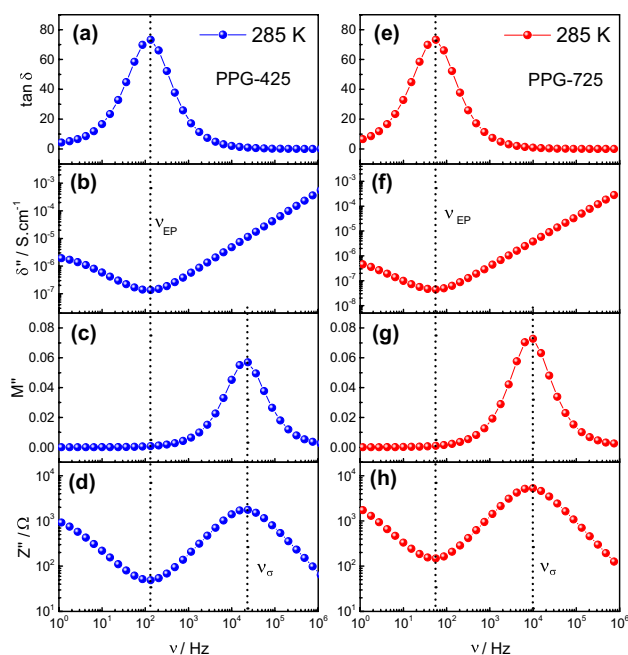


**Fig. 7** Comparison of frequency dependence of loss tangent (tan δ), imaginary parts of ac conductivity (σ″), electrical modulus (M″), and complex impedance (Z″) of PPG-425 and PPG-725 at a temperature $T = 285$ K

The temperature-dependent ionic conductivity relaxation times ($\tau_\sigma$) for PPG-425 and PPG-725 obtained from the above equation are presented in Fig. 5 along with the time constant of structural relaxation ($\tau_\alpha$) and viscosity ($\eta$) data regenerated from Singh et al. [26] and Lovrinic [48] for PPG-425, respectively, in the same temperature interval. The data of structural relaxation times of PPG-725 at the same temperature interval obtained from Koda et al. [27] are also included in panel 'b' of Fig. 5. The time constant of ionic conductivity ($\tau_\sigma$) follows the Arrhenius type temperature dependence of the form given in Eq. 6. The Arrhenius fitting parameters corresponding to $\tau_\sigma$, $\tau_\alpha$, and $\eta$ are as follows. $\tau_\sigma$: $\log_{10} A = -13.75$, $-13.37$, $E_{\tau(\sigma)} = 49.7 \pm 1.5$ kJ/mol, $49.6 \pm 1.3$ kJ/mol; $\tau_\alpha$: $\log A = -16.61$, $-16.97$, $E_{\tau(\alpha)} = 43.04 \pm 0.8$ kJ/mol, $46.3 \pm 0.3$; $\eta$: $\log A = -5.76$, $E_\eta = 43.7 \pm 1$ kJ/mol for PPG-425 and PPG-725, respectively. The results compiled in Fig. 5 indicate that the time constant of ionic conductivity or ionic conductivity relaxation time ($\tau_\sigma$) is somewhat slower than that of the corresponding reported structural relaxation time ($\tau_\alpha$) of both PPG. In addition, the activation energy of ionic conductivity relaxation time ($\tau_\sigma$) is higher than that of the activation energy of structural relaxation time ($\tau_\alpha$) as well as the

activation energy obtained from the viscosity data (compare Fig. 5a, b, c). The ratios of the activation energies of dc conductivity ($\sigma_{dc}$) and ionic conductivity relaxation time ($\tau_\sigma$) to that of structural relaxation time ($\tau_\alpha$) and viscosity ($\eta$) are 1.06 and 1.15, and 1.05 and 1.14, respectively, for PPG-425. Similarly for PPG-725, the ratio of $E_{\sigma(dc)}/E_{\tau(\alpha)} = 1.02$ and $E_{\tau(\sigma)}/E_{\tau(\alpha)} = 1.07$ have been obtained. An almost similar characteristic was also observed by Świergiel et al. [36] in a diluted electrolyte solution of propylene carbonate and lithium perchlorate.

It has been observed that impedance spectroscopy is one of the most widely used techniques to study the dc electrical conductivity and conductivity relaxation dynamics [33–36]. Therefore, the representative data in the form of real (Z′) and imaginary (Z″) parts of complex impedances are presented in Fig. 6 at different temperatures for pure PPG-425. The results presented in Fig. 6 indicate that the real part of impedance, Z′(ν) values initially remain constant with an increase of frequency and then decrease sharply in the high-frequency region, whereas the imaginary part of impedance spectra, Z″(ν) decrease slightly in low-frequency region and reach a minimum value, and above these frequencies, their values increase until display conductivity relaxation process in the high-frequency region. The dip exhibited in the Z″(ν) spectra in the low-frequency region are due to the presence of electrode polarization and the relaxation peaks observed towards the high-frequency side correspond to
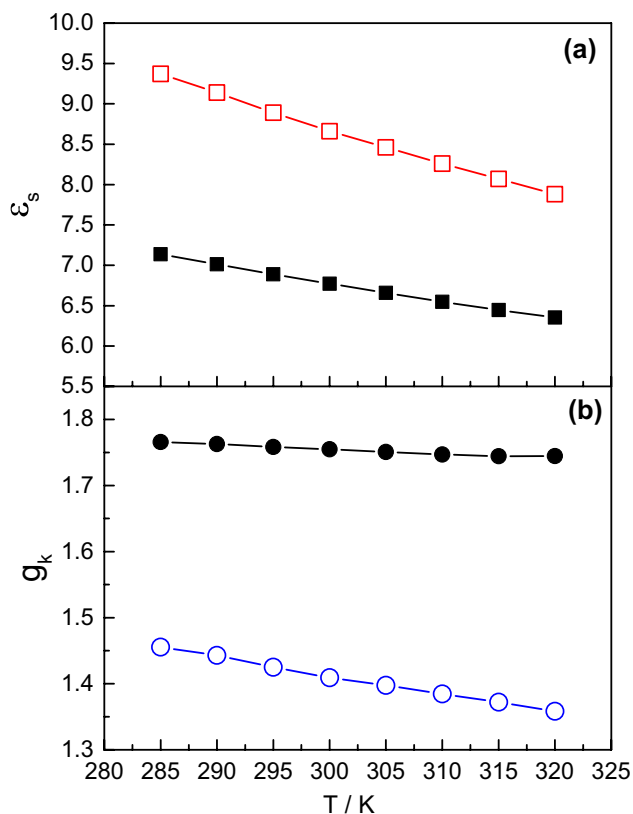
**Fig. 8** The temperature variation of **a** static permittivity, $\varepsilon_s$ **b** Kirkwood correlation factor ($g_k$) of both PPGs. Here, open symbol in each panel represents the data of PPG-425 while a solid symbol corresponds to PPG-725



**Fig. 9** Variation of dc ionic conductivity ($\sigma_{dc}$) and conductivity relaxation time ($\tau_\sigma$) with respect to viscosity ($\eta$) in panel **a** and structural relaxation time ($\tau_\alpha$) in panel **b** for PPG-425. Panel **c** shows the variation of dc ionic conductivity ($\sigma_{dc}$) and conductivity relaxation time ($\tau_\sigma$) as a function of structural relaxation time ($\tau_\alpha$) for PPG-725

the conductivity relaxation process. Interestingly, in both PPGs viz. PPG-425 and PPG-725, the magnitude of relaxation peak and dip in the $Z''(\nu)$ spectrum decrease with the increase in temperature. This signifies that with the help of $Z''(\nu)$ spectra, one can investigate both the effect of electrode polarization and the conductivity relaxation process simultaneously.

To clarify the importance of impedance spectra, relaxation processes are further analyzed in the comparative diagram of various dielectric and electrical formalisms of both PPGs drawn in Fig. 7 at a fixed temperature of 285 K. This figure displays that the minimum positions of $\sigma''(\nu)$ and $Z''(\nu)$ spectra are exactly lying at the same frequency at which the loss tangent (tan δ) spectra exhibit relaxation peak corresponding to the effect of electrode polarization. Further, a maximum point in $M''(\nu)$ and $Z''(\nu)$ spectra is showing up at the same frequency which relates to the ionic conductivity relaxation process. Consequently, from this figure, it tends to be inferred that the $Z''(\nu)$ spectra explore both the electrode polarization dynamics and conductivity relaxation processes over the frequency range in which tan δ, $\sigma''(\nu)$, and $M''(\nu)$ reveal only one relaxation process. For example,

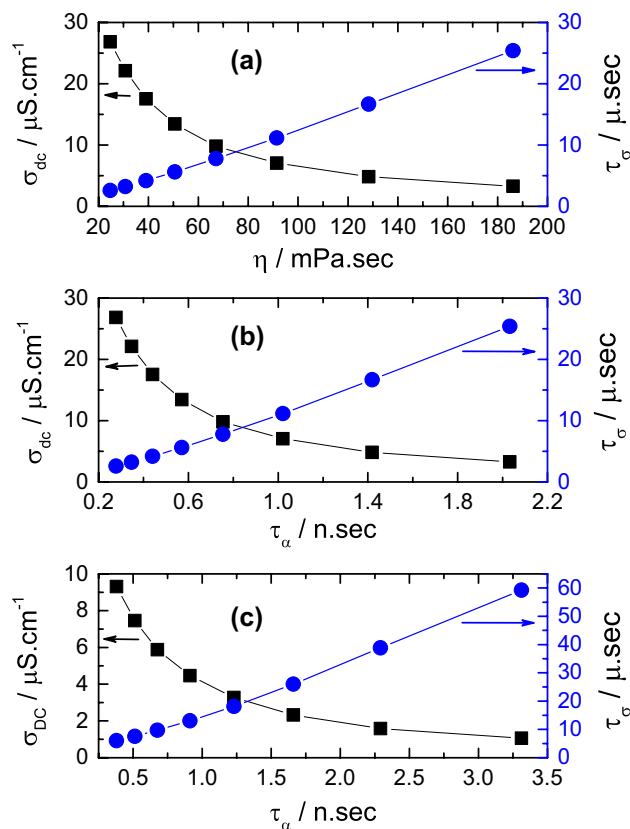tan δ and $\sigma''(\nu)$ display the relaxation mechanism due to the effect of electrode polarization, while $M''(\nu)$ exhibits only conductivity dynamics in the measured frequency range. It is also interesting to see that the values of ionic conductivity relaxation time ($\tau_\sigma$) obtained from the impedance spectra ($Z''$) are the same as those obtained from electrical modulus ($M''$) spectra for pure PPG. This could be related to the behavior of static permittivity ($\varepsilon_s$) which is linked by the relation $\sigma_{dc}.\tau_\sigma = \varepsilon_0.\varepsilon_s$ [28]. It is noted that the values of dc conductivity ($\sigma_{dc}$) at different temperatures obtained from this relation are the same as the values obtained from the plateau region that exists in the spectra of the real part of ac electrical conductivity ($\sigma'$). This relationship suggests that the complex impedance and electrical modulus often follow the Debye-type relaxation behavior in the static permittivity frequency regime of the Ohmic conducting dielectric materials, and for such a system the conductivity relaxation time can be calculated by knowing the values of static permittivity ($\varepsilon_s$) and dc conductivity ($\sigma_{dc}$) of the material. To investigate the behavior of dipoles in the measured temperature range in pure PPG, the Kirkwood correlation factor ($g_k$)

values were estimated at different temperatures using the Kirkwood–Fröhlich equation given by [49]

$$g_K = \left(\frac{9k_B T \varepsilon_0 M}{\rho N_A \mu^2}\right) \cdot \left[\frac{(\varepsilon_s - \varepsilon_\infty)(2\varepsilon_s + \varepsilon_\infty)}{\varepsilon_s(\varepsilon_\infty + 2)^2}\right] \qquad (10)$$

With $N_A$ being the Avogadro number, $\rho$ the density, M the molecular mass, $k_B$ the Boltzmann's constant, $\varepsilon_0$ the permittivity in free space, and $\varepsilon_s$ representing the static permittivity. We used the static permittivity ($\varepsilon_s$) values obtained from the present study and high-frequency limiting permittivity ($\varepsilon_\infty$) was calculated from the refractive index ($\varepsilon_\infty = 1.05\, n_D^2$), while the dipole moment $\mu$ (3.5 D) [50] and the temperature-dependent values of density are taken from the literature [48, 50]. The temperature dependence of static permittivity ($\varepsilon_s$) and Kirkwood correlation factor ($g_k$) values of both PPGs are presented in Fig. 8. This figure clearly shows that
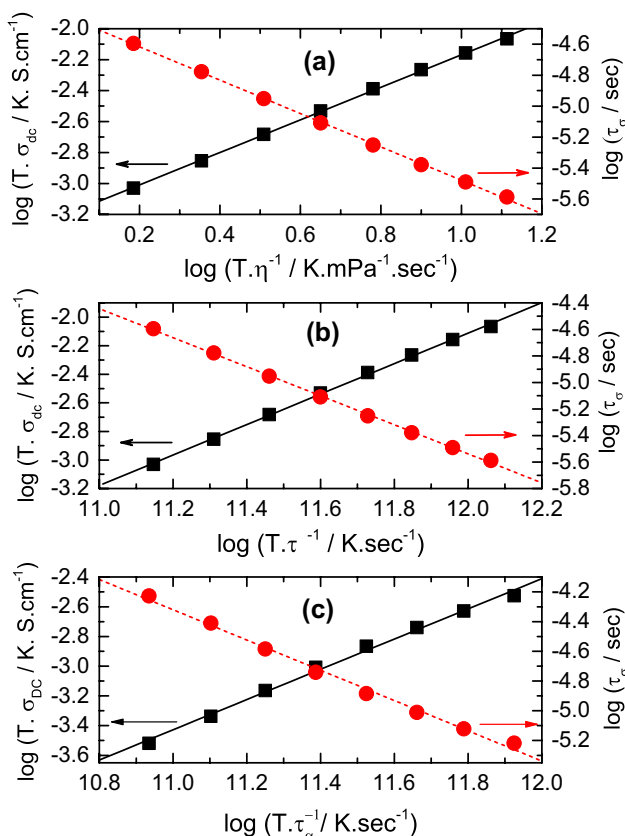


**Fig. 10 a** Stokes–Einstein–Nernst plot for PPG-425. The dashed and solid line drawn in the figure has a slope of − 1.07 ± 0.01 and 1.05 ± 0.01, respectively. **b** Stokes–Einstein–Debye plot for PPG-425. The dashed and solid line drawn in the figure has a slope of − 1.08 ± 0.01 and 1.06 ± 0.01, respectively. **c** Stokes–Einstein–Debye plot for PPG-725. The dashed and solid line drawn in the figure has a slope of − 1.02 ± 0.01 and 1.01 ± 0.01, respectively

both physical quantities, viz., $\varepsilon_s$ and $g_k$ values decrease with the increase of temperature for both PPGs. However, this behavior is more noticeable in low molecular weight polymers, i.e., PPG-425. This suggests that PPG-725 has a high degree of polymerization as compared to PPG-425 and hence showed a lower value of static permittivity. Previously, Park et al. [21] and Ikada et al. [23, 24] reported identical findings for the propylene glycol oligomers. Furthermore, the linear decrease of static permittivity ($\varepsilon_s$) with an increase of temperature following Curie law temperature dependence is usually found in most dipolar liquids. Similarly, the Kirkwood correlation factor ($g_k$) value in the molecular structure of both PPGs slightly decreases with an increase in temperature, suggesting the antiparallel ordering of the dipoles. This behavior is consistent with the previous results of the creation of a compact structure [50, 51] due to a high degree of polymerization with a dipole moment smaller than that of a free monomer.

Figure 9 presents the variation of dc conductivity ($\sigma_{dc}$) and ionic conductivity relaxation time ($\tau_\sigma$) as a function of viscosity ($\eta$) in the panel 'a' for PPG-425 and as a function of structural relaxation time ($\tau_\alpha$) in panel 'b' and 'c' for pure PPG-425 and PPG-725, respectively. The solid and dashed lines drawn in the panel 'a' of this figure represent the best fits to the experimental data for the function [36], $\sigma_{dc} \propto \eta^{-m}$ or $\tau_\sigma \propto \eta^m$ with the determined exponent values 1.01 and 1.15, respectively, for PPG-425. Similarly, the solid and dashed lines drawn in the panel 'b' and 'c' of this figure represent the best fits to the experimental data for the function [36], $\sigma_{dc} \propto \tau_\alpha^{-m}$ or $\tau_\sigma \propto \tau_\alpha^m$ with the determined exponent values 1.02 and 1.18 for PPG-425, and 0.96 and 1.13 for PPG-725, respectively. These values are very close to the relation between the partners' corresponding activation energies as discussed earlier, i.e., $E_{\sigma(dc)}/E_{\tau(\alpha)} = 1.06$ and $E_{\tau(\sigma)}/E_{\tau(\alpha)} = 1.15$, and $E_{\sigma(dc)}/E_\eta = 1.05$ and $E_{\tau(\sigma)}/E_\eta = 1.14$, respectively, for PPG-425 and $E_{\sigma(dc)}/E_{\tau(\alpha)} = 1.02$ and $E_{\tau(\sigma)}/E_{\tau(\alpha)} = 1.07$ for PPG-725, respectively. Further, this figure identifies that dc electrical conductivity ($\sigma_{dc}$) exponentially decreases, whereas the ionic conductivity relaxation time ($\tau_\sigma$) increases nonlinearly with the increase of structural relaxation time ($\tau_\alpha$) or viscosity ($\eta$) of pure PPG. Almost similar behavior was also seen in the variation of $\sigma_{dc}$ and $\tau_\sigma$ as a function of viscosity ($\eta$) in pure propylene carbonate [35] and its electrolyte solutions [36]. Therefore, it seems to be interesting to consider the Stokes–Einstein–Nernst relationship [35, 36, 44, 45] of the form $\sigma_{dc}.T \propto T/\eta$ or $\tau_\sigma \propto \eta/T$ and the Stokes–Einstein–Debye relationship [36, 44, 45] of the form $\sigma_{dc}.T \propto T/\tau_\alpha$ or $\tau_\sigma \propto \tau_\alpha/T$ for pure PPG for the interpretation of experimental data relating to the movement of ions in viscous media.

Figure 10 displays the Stokes–Einstein–Nernst [36, 44, 45] plot in the form of $\sigma_{dc}.T$ versus $\eta/T$ and $\tau_\sigma$ versus $\eta/T$

in a log–log scale in panel 'a'. Similarly, panel 'b' displays the Stokes–Einstein–Debye [36, 44, 45] plot in the form of $\sigma_{dc}.T$ versus $\tau_\alpha/T$ and $\tau_\sigma$ versus $\tau_\alpha/T$ in a log–log scale. The solid and dashed lines depicted along with the data in the panel 'a' and 'b' of this figure represent the slope of $-1.07\pm0.01$, $1.05\pm0.01$ and $-1.08\pm0.01$, $1.06\pm0.01$, respectively for PPG-425. Similarly, the solid and dashed lines drawn along the data in panel 'c' represent the slope of $-1.02\pm0.01$ and $1.01\pm0.01$, respectively, for PPG-725. Clearly, in the log–log scale, the experimental data show linear dependence with a slope closer to the unity thus fulfilling the Stokes–Einstein–Nernst/Stokes–Einstein–Debye relation quite well. It means that the dimension of the molecular medium in which ion movements take place does not depend on temperature. Surprisingly, the behavior of the above-mentioned physical quantities and their slopes are similar to those reported in lithium percolate ($LiClO_4$) electrolyte solutions in PPG solvents [39]. This demonstrates that the electrical conduction behavior of unknown ions impurities existing in pure PPG and extremely low known concentration added ions in pure PPG is the same. We may also deduce that at the reported temperature range, the translation ionic movements are closely coupled with the orientational molecular motions for PPG. This suggests that the size of the ion in polymer electrolytes is significantly less than the size of the solvent molecule, viz., polymer. As a result, the local "microscopic" viscosity should regulate charge transfer rather than the macroscopic viscosity [39], which is determined by the overall motion of the polymer chain. In simpler words, the rate of segmental or structural rearrangements should be used to characterize the rate of ion transport mechanism in polymers. However, it is obvious that we still have a lot to learn about the connection between ionic transport and polymer segmental relaxation, thus a thorough examination appears warranted.

## 4 Summary and conclusion

The detailed results on electrical and dielectric dispersion of pure poly(propylene glycol) (PPG) in the frequency range from 1 Hz to 1 MHz and the temperatures from 285 to 320 K are presented. Based on the comparative analysis of different forms of spectra, it was identified that impedance representation (Z″ spectra) explores both the electrode polarization dynamics and conductivity relaxation processes over the frequency ranges in which tan δ, σ″(ν), and M″(ν) have revealed only one relaxation process. The imaginary parts of impedance (Z″) and modulus (M″) dispersion curves of both poly(propylene glycol) (PPG-425, PPG-725) show the same value of conductivity relaxation time in their respective data representation. It was found that the static permittivity decreases with an increase in temperature for both

studied polymers. However, PPG-725 shows a lesser value of static permittivity as compared to PPG-425 at the same temperature suggesting a high degree of polymerization exists in PPG-725. Moreover, the temperature dependence of the Kirkwood correlation factor identifies that PPG prefers a compact structure with lesser dipole moment as compared to a free monomer. Further, it has been observed that on a double logarithmic scale, the dependence of dc conductivity ($\sigma_{dc}$) on the structural relaxation time ($\tau_\alpha$) or viscosity of both PPGs shows a linear behavior with negative slope closure to the unity, thus satisfying the Stokes–Einstein–Debye/Stokes–Einstein–Nernst relationship quite well. This suggests that the translation ionic movements are closely coupled with the orientational molecular motions for PPG.

## References

1. G. Williams, Trans. Faraday Soc. **61**, 1564 (1965)
2. M.E. Baur, W.H. Stockmayer, J. Chem. Phys. **43**, 4319 (1965)
3. S. Yano, R.R. Rahalkar, S.P. Hunter, C.H. Wang, R.H. Boyd, J. Polym. Sci. Polym. Phys. Ed. **14**, 1877 (1976)
4. M.S. Beevers, D.A. Elliott, G. Williams, Polymer **20**, 785 (1979)
5. M.S. Beevers, D.A. Elliott, G. Williams, Polymer **21**, 13 (1980)
6. K. Vardarajan, R.F. Boyer, Polymer **23**, 314 (1982)
7. G.P. Johari, Polymer **27**, 866 (1986)
8. K. Pathmanathan, G.P. Johari, Polymer **29**, 303 (1988)
9. S.P. Anderson, O. Andersson, Macromolecules **31**(9), 2999 (1988)
10. D. Engberg, J. Schuller, B. Strube, A.P. Sokolov, L.M. Torell, Polymer **40**, 4755 (1999)
11. T. Alper, A.J. Barlow, R.W. Gray, Polymer **17**, 665 (1976)
12. A.J. Barlow, A. Erginsav, Polymer **16**, 110 (1975)
13. J. Cochrane, G. Harrison, J. Lamb, D.W. Phillips, Polymer **21**, 837 (1980)
14. T.M. Connor, D.J. Blears, G. Allen, Trans. Faraday Soc. **61**, 1097 (1965)
15. K. Kabara, V. Madhurima, A.C. Kumbharkhane, A.V. Sarode, Mater. Chem. Phys. **209**, 16 (2018)
16. S.W. Smith, B.D. Freeman, C.K. Hall, Macromolecules **30**(7), 2052 (1997)
17. D.R. Jones, C.H. Wang, J. Chem. Phys. **65**(5), 1835 (1976)
18. A. Suzuki, M. Masuko, K. Wakisaka, Tribiol Int **35**, 55 (2002)
19. R.J. Sengwa, R. Choudhary, K. Kaur, Polym. Int. **49**, 1308 (2000)
20. I.S. Park, K. Saruta, S. Kojima, Mol. Cryst. Liq. Cryst. **322**, 329 (1998)
21. I.S. Park, K. Saruta, S. Kojima, J. Phys. Soc. Jpn **67**(12), 4131 (1998)
22. J. Swenson, D. Engberg, W.S. Howells, T. Seydel, F. Juranyi, J. Chem. Phys. **122**(24), 244702 (2005)
23. E. Ikada, H. Fukushima, T. Watanabe, J. Polym. Sci. Polym. Phys. Ed. **17**, 1789 (1979)
24. I. Ikada, M. Ashida, Colloid Polym. Sci. **264**, 602 (1986)
25. K. Grzybowska, A. Grzybowski, J. Zioło, M. Paluch, S. Capaccioli, J. Chem Phys. **125**, 044904 (2006)
26. L.P. Singh, S. Cerveny, A. Alegría, J. Colmenero, J. Phys. Chem. B **115**, 13817 (2011)

27. S. Koda, T. Shibata, I.S. Park, S. Kojima, Curr. Appl. Phys. **15**, 805 (2015)

28. F. Kremer, A. Schönhals, *Broadband Dielectric Spectroscopy* (Springer-Verlag, Berlin, 2003)

29. P.B. Ishai, M.S. Talary, A. Caduff, E. Levy, Y. Feldman, Meas. Sci. Technol. **24**, 102001 (2013)

30. R.J. Klein, S. Zhang, S. Dou, B.H. Jones, R.H. Colby, J. Runt, J. Chem. Phys. **124**, 144903 (2006)

31. D. Reuter, K. Seitz, P. Lunkenheimer, A. Loidl, J. Chem. Phys. **153**, 014502 (2020)

32. G. Power, J.K. Vij, G.P. Johari, J. Phys. Chem. B **111**, 11201 (2007)

33. J. Jadżyn, J. Świergiel, Ind. Eng. Chem. Res. **51**, 807 (2012)

34. J. Świergiel, L. Bouteiller, J. Jadżyn, Ind. Eng. Chem. Res. **52**, 11974 (2013)

35. R.J. Sengwa, S. Choudhary, P. Dhatarwal, J. Mol. Liq. **225**, 42 (2017)

36. J. Świergiel, I. Płowaś, J. Jadżyn, Ind. Eng. Chem. Res. **54**, 2108 (2015)

37. S. Choudhary, R.J. Sengwa, Indian J. Eng Mater. Sci. **19**, 245 (2012)

38. J. Świergiel, I. Płowaś, J. Grembowski, J. Jadżyn, J. Chem. Eng. Data **60**, 3588 (2015)

39. Y. Wang, F. Fan, A.L. Agapov, T. Saito, J. Yang, X. Yu, K. Hong, J. Mays, A.P. Sokolov, Polymer **55**, 4067 (2014)

40. J. Świergiel, J. Jadżyn, J. Phys. Chem. B **113**, 14225 (2009)

41. J.K. Park, J.C. Ryu, W.K. Kim, K.H. Kang, J. Phys. Chem. B **113**, 12271 (2009)

42. I. Płowaś, J. Świergiel, J. Jadżyn, J. Electrochim, Acta **178**, 511 (2015)

43. G. Stokes, Trans. Cambridge Philos. Soc. **9**, 5 (1856)

44. J.P. Hansen, J.R. McDonald, *Theory of Simple Liquids* (Academic Press, New York, 1991)

45. G.P. Johari, O. Andersson, J. Chem. Phys. **125**, 124501 (2006)

46. A. D. Acharya, S. Sharma, Ginni, S. Bisoyi, M. Ahmad, L. P. Singh, and S. S. Manhas, J. Phys.: Conf. Ser. 1531, 012025 (2020).

47. N.E. Hill, W.E. Vaughan, A.H. Price, M. Davies, *Dielectric Properties and Molecular Behaviour* (Van Nostrand Reinhold, London, 1969)

48. Spencer Lovrinic, "Physicochemical study of poly(propylene glycol)-water binary mixture" Science Research distinction thesis, The Pennsylvania State University, (2016).

49. H. Fröhlich, *Theory of Dielectrics* (Clarendon, Oxford, 1958)

50. G.P. Johari, W. Danhauser, J. Chem. Phys. **48**, 5114 (1968)

51. L.P. Singh, R. Richert, Phys. Rev. Lett. **109**, 167802 (2012)